

Platelet-Rich Plasma Attenuates Knee Osteoarthritis in Rats via Modulation of Gut Microbiota

Dongmei Yan*, Qishan Li*, Mengjie Wang, Yaochi Nie, Xueyuan Sun, Lin Na, Hui Wang 

Department of Blood Transfusion, the Second Affiliated Hospital of Harbin Medical University, Harbin, Heilongjiang Province, People's Republic of China

*These authors contributed equally to this work

Correspondence: Hui Wang, Department of Blood Transfusion, the Second Affiliated Hospital of Harbin Medical University, No. 246, Xuefu Road, Nan'gang District, Harbin, Heilongjiang Province, 150000, People's Republic of China, Email wanghui@hrbmu.edu.cn

Background: Platelet-rich plasma (PRP), a platelet and plasma concentrate extracted from whole blood via centrifugation, has multiple bioactive properties. However, its role in the progression of knee osteoarthritis (KOA) and the underlying mechanisms of action remain unclear. In this study, we investigated the therapeutic effects of PRP extracted from rat whole blood on the progression of KOA and assessed whether its mechanism involves modulation of the gut microbiota (GM).

Methods: Knee osteoarthritis (KOA) rat models were established by intra-articular injection of 1 mg of sodium monoiodoacetate (MIA) into the knee joints. The rats were administered intra-articular injections of 60 μ L of PRP on days 15, 17, and 19 post-modeling. Moreover, we established pseudo-germ-free (pGF) KOA rat models and performed fecal microbiota transplantation (FMT) experiments to investigate whether the GM mediates the therapeutic effects of PRP on KOA. Therapeutic efficacy was assessed by conducting gait analysis, joint swelling measurement, and micro-CT scanning. The pathological changes were evaluated via Safranin O-Fast Green and hematoxylin-eosin (HE) staining, as well as immunohistochemistry (IHC). The alterations in the GM were evaluated by 16S rRNA gene sequencing.

Results: We found that PRP effectively improved abnormal gait patterns, reduced inflammation levels, alleviated subchondral bone loss, repaired the damaged articular surface, and mitigated cartilage destruction in KOA rats. Concurrently, PRP intervention restored intestinal barrier function and positively modulated the dysregulated composition of the GM. The pGF condition reversed the improvements induced by PRP in KOA rats, whereas transplanting GM from PRP-treated KOA rats to recipient KOA rats promoted recovery in the latter.

Conclusion: This study demonstrated that PRP ameliorates KOA progression, at least partially, by modulating GM diversity (notably *Ligilactobacillus murinus*), enhancing intestinal barrier integrity, and reducing systemic inflammation.

Keywords: platelet-rich plasma, gut microbiota, knee osteoarthritis, fecal microbiota transplantation

Introduction

Knee osteoarthritis (KOA) is a prevalent degenerative joint disease characterized primarily by the degeneration of articular cartilage, the formation of osteophytes, and damage to the subchondral bone. It greatly contributes to functional impairment and socioeconomic burden among the elderly population.¹ As populations around the world keep getting older, the prevalence of KOA continues to increase. Clinical management of KOA follows a guideline-recommended approach, prioritizing non-pharmacological strategies (such as physical therapy, exercise, and weight management) as first-line interventions, while also incorporating pharmaceutical options including NSAIDs, analgesics, and corticosteroids.² However, these therapeutic approaches have several limitations: NSAIDs may cause gastrointestinal, cardiovascular, and renal adverse reactions;³ opioid analgesics demonstrate effective pain relief but carry significant risks of addiction;⁴ and intra-articular hyaluronic acid injections offer short-lived efficacy and incur substantial costs,

restricting their clinical applicability.⁵ Consequently, safe and effective novel treatment strategies need to be urgently developed for managing KOA.

Platelet-rich plasma (PRP) is a high-concentration platelet concentrate obtained by centrifuging autologous whole blood, which is significantly enriched with multiple growth factors, cytokines, and bioactive proteins compared to simple plasma or serum preparations. Critically, effective repair and regeneration of damaged articular cartilage and subchondral bone in KOA remain challenging with conventional approaches. PRP has emerged as a promising regenerative therapy, offering a potent combination of anti-inflammatory, anabolic, and pro-healing signals that are often insufficient in standard autologous plasma concentrates. It has been widely applied in recent years in the fields of tissue repair and regenerative medicine, including wound healing, orthopedic diseases, and sports injuries.⁶ Specifically for KOA, PRP can promote the proliferation of chondrocytes, stimulate cartilage matrix synthesis, suppress the expression of inflammatory factors, and increase the proliferation and differentiation of bone marrow mesenchymal stem cells (BMSCs), thereby playing a therapeutic role in treating KOA. Additionally, when PRP and its derivatives were used to treat chondrocytes in vitro, they promoted cartilage regeneration and suppressed inflammatory responses in cartilage tissue.^{7,8} These multifaceted actions position PRP not merely as a symptom modulator but as a potential disease-modifying agent capable of addressing the structural deterioration central to KOA pathogenesis. Moreover, the intra-articular injection dose of PRP used in preclinical rodent models, typically ranging from 30 to 60 μL per joint, has been established to be safe and effective in mitigating KOA progression.^{9–11} However, the mechanisms underlying the therapeutic effects of PRP on KOA, particularly its systemic effects, remain incompletely understood.

The gut microbiota (GM) and its metabolites play crucial roles in regulating systemic inflammation and osteoarticular health.¹² Compromised integrity of the intestinal barrier and dysbiosis may contribute to the onset and progression of KOA through multiple pathways, including the regulation of ferroptosis, metabolic disorders, and immune abnormalities.^{13,14} The gut microenvironment is a metabolically complex and active microbial ecosystem that plays an important role in maintaining host homeostasis and health.¹⁵ Transplanting the fecal microbiota from metabolically impaired human donors accelerates the progression of osteoarthritis in mice.¹⁶ Moreover, probiotics such as *Lactobacillus acidophilus* can mitigate osteoarthritis-associated pain, cartilage disintegration and GM dysbiosis in an experimental murine OA model.¹⁷ These findings indicate that the GM may serve as a novel therapeutic target for KOA intervention.

Some researchers have highlighted the presence of a bidirectional “gut-joint axis”, wherein immune, inflammatory, and metabolic signals link intestinal health to joint homeostasis.¹⁸ This finding suggests that intra-articular PRP may exert systemic effects via this axis. Therefore, we hypothesized that PRP alleviates KOA not only locally but also by modulating the GM and intestinal barrier. To test this hypothesis, we combined a rat KOA model with pseudo-germ-free (pGF) and fecal microbiota transplantation (FMT) approaches and 16S rRNA gene sequencing and short-chain fatty acids (SCFAs) analysis. We aimed to determine whether PRP protects against KOA via GM remodeling, offering new insights for its clinical application.

Materials and Methods

Animals and the Preparation of PRP

Specific pathogen-free (SPF)-grade male Sprague Dawley (SD) rats (n =72; age: eight weeks old; weight: 180–200 g) were purchased from SPF Biotechnology Co., Ltd. (Beijing, China; license number: SCXK (Jing) 2024–0001). This study was approved by the Animal Ethics Committee of The Second Affiliated Hospital of Harbin Medical University (Ethics Approval Number: SYDW2024-059). All animal experiments were conducted strictly following our institution’s Guidelines for the Care and Use of Laboratory Animals and were reported following the ARRIVE guidelines.¹⁹

All rats were maintained under SPF conditions with a 12-h/12-h light/dark cycle and provided ad libitum access to food and water. After acclimation for one week, PRP was isolated as previously described by Yan et al¹¹ Briefly, the rats were anesthetized via intraperitoneal injection of 50 mg/kg pentobarbital sodium. Whole blood was collected via abdominal aortic puncture in anticoagulant tubes containing sodium citrate; these blood samples were centrifuged 2,000 $\times g$ for 10 min at 4 $^{\circ}\text{C}$ to obtain the initial PRP. Platelet counts in whole blood and PRP were measured using

an automated hematology analyzer. The initial platelet concentration in the PRP was 3.7 times greater than the baseline level. Then, the initial PRP was activated through sequential freezing at -80°C for 24 h and incubation at 37°C for 1 h. Activated PRP was centrifuged at $12,000 \times g$ for 2 min at 4°C to remove debris, and the supernatant was collected and stored at -80°C for subsequent use.

Animals and Group Treatments

KOA Model

After one week of acclimatization, a separate group of rats received a single intra-articular injection of 1 mg of sodium monoiodoacetate (MIA) (Cat: HY-D0849, MCE, New Jersey, USA) in normal saline into the left knee joint to induce KOA. The rats in the control group received an equivalent volume of normal saline. The animals were maintained for another 14 days. The emergence of touch-evoked pain and hyperalgesia was considered to indicate successful modeling.²⁰ The rats were subsequently divided into four groups ($n = 6/\text{group}$): (I) Control group: knee joints were injected with an equivalent volume of normal saline; (II) KOA group: knee joints were injected with an equivalent volume of normal saline; (III) PRP group: intra-articular injections of $60 \mu\text{L}$ of PRP were administered into the knee joint on days 15, 17, and 19 after MIA injection.¹¹ (IV) diclofenac sodium (DCF) group: oral administration of 5 mg/kg diclofenac sodium (Cat No: HY-15037; MCE, New Jersey, USA) once daily starting from day 15 after MIA injection. All animals were maintained for another 14 days. After behavioral testing, the animals were euthanized via the inhalation of an overdose of CO_2 . Fecal samples and knee joint tissues were collected for subsequent experiments.

Establishment of a Pseudo-Germ-Free Knee Osteoarthritis (pGF-KOA) Rat Model

After one week of adaptive feeding, pGF rats were established.²¹ All rats were administered drinking water containing 0.5 g/L vancomycin, 1 g/L neomycin sulfate, 1 g/L metronidazole, and 1 g/L ampicillin for 15 consecutive days. The results of 16S rRNA analysis demonstrated significantly reduced richness (Chao1 index) and diversity (Shannon index) of the GM, confirming that the pGF rat model was successfully established. The term “pGF” refers to a state in which the GM has been greatly depleted by broad-spectrum antibiotic cocktail treatment, not complete sterility.

Initially, pGF rats were used to establish the pGF-KOA rat model via intra-articular MIA injection as previously described, followed by treatment with PRP. Antibiotic treatment was administered throughout the experimental period to maintain the pGF state. The animals were subsequently divided into three groups ($n = 6/\text{group}$): (I) the pGF group, (II) the pGF-KOA group, and (III) the pGF-PRP group. All animals were continuously housed for four weeks with concurrent antibiotic treatment. After behavioral testing, the rats were euthanized via inhalation of an overdose of CO_2 . Fecal and knee joint tissues were collected for subsequent experiments.

Fecal microbiota transplantation (FMT): To evaluate the effect of FMT on joints, fresh fecal samples were first collected from rats in the control, KOA, PRP, and DCF groups for preparing fecal bacterial suspensions. Fecal samples collected from donor rats in each group were pooled, homogenized under anaerobic conditions with sterile phosphate-buffered saline (PBS; 100 mg feces/mL), subsequently filtered through sterile mesh, and centrifuged to obtain bacterial pellets.²¹ The pellets were resuspended in PBS containing 20% glycerol and stored at -80°C for future use.

Subsequently, a pGF-KOA rat model was established following the described method, and the rats were randomly divided into five groups ($n = 6$ rats per group): (I) the control-FMT group, in which the rats received an oral gavage of fecal bacteria (0.42 g/kg) from the control group; (II) the KOA group, in which the rats received an oral gavage of an equivalent volume of saline; (III) the KOA-FMT group, in which the rats received an oral gavage of fecal bacteria (0.42 g/kg) from the KOA group; (IV) the PRP-FMT group, in which the rats received an oral gavage of fecal bacteria (0.42 g/kg) from the PRP group; and (V) the DCF-FMT group, in which the rats received an oral gavage of fecal bacteria (0.42 g/kg) from the DCF group. The rats in each group were subjected to oral gavage three times per week for four weeks.²² Antibiotic treatment was withdrawn 48 h before the first FMT gavage and was not administered during the FMT period to allow microbial engraftment. After the experiment ended, all rats underwent behavioral testing, followed by euthanasia via an overdose of CO_2 . Then, fecal samples and knee joint tissues were collected for subsequent analysis.

Gait Analysis and Swelling Measurement

Under calm conditions, the hind paws of the rats were immersed in red ink, and then the rats were allowed to walk on white paper covering a 7 cm-wide filler to obtain their footprints. Stride length and foot intensity of pressure were analyzed using a computerized gait analysis system. To measure joint swelling, the joint circumference of the rats was assessed using a tape measure under anesthesia while with the knee joint fixed at 120° of flexion and the ankle joint in full extension.²¹

Micro-CT Scanning

Knee joints fixed in 4% paraformaldehyde were scanned using a SkyScan1276 scanner (Bruker, Massachusetts, USA). Three-dimensional reconstruction was performed using the reconstruction system. For quantitative analysis, the following standard three-dimensional morphometric parameters of the subchondral bone were measured or calculated by the instrument's analysis software: bone mineral density (BMD), bone volume fraction (BV/TV), trabecular thickness (Tb.Th), trabecular separation (Tb.Sp), and structural model index (SMI).

Histopathological Analysis

Colon tissues and decalcified knee joints fixed in 4% paraformaldehyde were dehydrated, embedded, and sectioned. Hematoxylin and eosin (H&E) staining was performed on both knee joints and colon tissues to observe histomorphological changes. Safranin O-fast green staining was conducted on the knee joint tissues. Articular cartilage and synovium were evaluated using the Osteoarthritis Research Society International (OARSI) scoring system and synovitis scoring criteria, respectively, to assess the progression of knee lesions and the inflammatory status.^{23,24}

Immunohistochemistry (IHC) Analysis

For IHC staining, knee joint and colon tissue sections underwent antigen retrieval and blocking procedures. Knee joint sections were incubated with collagen II antibody (1:200, Cat. No. A00517-2; Boster, Wuhan, China) and an α -SMA antibody (1:100, Cat. No. 14395-1-AP, RRID: AB_2223009; Sanying, Wuhan, China) Colon sections were incubated with occludin antibody (1:500, Cat. No. 27260-1-AP, RRID: AB_2880820) and ZO-1 antibody (1:500, Cat. No. 21773-1-AP, RRID: AB_10733242; Proteintech, Wuhan, China) All sections were incubated overnight at 4 °C. Subsequently, HRP-conjugated goat anti-rabbit secondary antibody (1:200, Cat. No. LJS-S-0001, GenScript, Wuhan, China) was added. DAB chromogenic solution was applied, and the nuclei were counterstained with hematoxylin. The sections were observed and photographed under an ECLIPSE Ci microscope (Nikon, Japan). The integrated optical density (IOD) of positively stained areas or positive cell ratios was evaluated using the ImageJ software.²⁵

16S rRNA Gene Sequencing

Microbial DNA was extracted from fecal samples using the TGuide S96 Magnetic Soil/Stool DNA Kit (DP812, Tiangen Biotechnology, Beijing, China). Subsequently, PCR amplification targeting the V3–V4 hypervariable region of the bacterial 16S rRNA gene was performed using primers 27F (5'-AGRGTGGATYNTGGCTCA G-3') and 1492R (5'-TASGGHTACCTTGTTASGACTT-3'), with sequencing adapters pre-added to the 5' ends. The amplification products were purified and quantified, pooled in equimolar ratios to construct sequencing libraries, and subjected to quality control. The libraries that passed quality control were sequenced on an Illumina NovaSeq 6000 platform using paired-end sequencing (2 × 250 bp). The obtained raw sequences were processed through the QIIME2 pipeline for bioinformatic analysis, including quality control, denoising, clustering into operational taxonomic units (OTUs) at 97% sequence similarity, and taxonomic annotation using the SILVA 138 and NT databases.

Short-Chain Fatty Acids (SCFAs) Analysis

For SCFAs analysis, fecal samples were processed and derivatized. Acetic acid, propionic acid, butyric acid, etc., were quantified using a 7890B-7000D gas chromatography-mass spectrometer (GC-MS; Agilent, California, US).

Statistical Analysis

All data were analyzed using SPSS 26.0 (version 26.0). Normality was determined by conducting the Shapiro–Wilk test. The differences among multiple groups were determined by conducting one-way analysis of variance (ANOVA) with Tukey's post hoc test. The results were expressed as the mean \pm SD and were considered to be statistically significant at $P < 0.05$. A sample size of $n = 6$ per group was used, based on prior KOA model studies, ensuring adequate power for our primary outcomes.

Results

Protective Effects of PRP on KOA Rats

To investigate the effect of PRP on KOA, we established a KOA rat model via a single intra-articular MIA injection, which induced a well-characterized early inflammatory osteoarthritic stage by the 4-week endpoint used in this study. Rats were subsequently treated with PRP. The experimental flowchart is illustrated in [Figure 1A](#). Pain is the most common symptom experienced by KOA patients. At this stage, gait alterations primarily reflect pain-related behavioral adaptations rather than late-stage structural joint changes. Therefore, gait measurement serves as a key behavioral method for the clinically significant assessment of KOA-related pain in this model. The results of gait analysis demonstrated that both PRP and DCF effectively restored gait abnormalities induced by KOA ([Figure 1B](#)), manifested as improvements in stride length ([Figure 1C](#)) and stride pressure ([Figure 1D](#)). These findings suggest that PRP may effectively decrease the level of pain experienced by individuals. Moreover, joint swelling was evaluated by measuring the knee joint circumference in the rats. Both PRP and DCF significantly alleviated knee joint swelling caused by injecting MIA ([Figure 1E](#)).

Imaging serves as a valuable method for the clinical assessment of KOA and provides the required evidence for clinical evaluation. Micro-CT analysis of knee joints across experimental groups revealed that the KOA rats had sparse and fragmented subchondral trabecular bone ([Figure 1F](#)). Significantly reduced values were observed for bone mineral density (BMD), bone volume fraction (BV/TV), and trabecular thickness (Tb.Th) ([Figure 1G–J](#)), whereas the structural model index (SMI) and trabecular separation (Tb.Sp) increased significantly ([Figure 1H and K](#)). Both PRP and DCF alleviated structural destruction and loss in the bone tissues of rats.

Articular cartilage damage serves as a primary diagnostic criterion for KOA patients and represents a widespread pathological manifestation in this population. After determining the role of PRP in modulating the phenotypes of KOA, we subsequently examined pathological changes in cartilage. Safranin O-fast green staining demonstrated that PRP and DCF effectively ameliorated superficial cartilage fibrillation and loss of proteoglycans in the knee joints of KOA rats, indicating significant reparative effects ([Figure 1L](#)). H&E staining revealed that both PRP and DCF interventions effectively reorganized the disordered chondrocyte population and improved the cartilage layer structure ([Figure 1M](#)). To histologically validate the protective effects of PRP on cartilage and its anti-inflammatory effects, we performed osteoarthritis scoring on the Safranin O-fast green staining results and synovitis scoring on the H&E staining results. We found that PRP and DCF interventions effectively decreased the osteoarthritis and synovitis scores in KOA rats ([Figure 1N and O](#)). To verify the regulatory effect of PRP on cellular fibrosis, we detected the level of expression of collagen II and α -SMA proteins in knee joint cartilage tissues through IHC. The results indicated that PRP and DCF altered the protein expression of collagen II and α -SMA in the cartilage tissues of KOA rats. Specifically, compared to the KOA group, PRP and DCF treatment increased the expression of collagen II (a key cartilage matrix component) and decreased the expression of α -SMA (a marker associated with fibrotic changes) ([Figure 1P–R](#)). These results indicate that PRP has a significant therapeutic effect on KOA rats.

Regulatory Effects of PRP on Intestinal Barrier and GM in KOA Rats

The pathogenesis of KOA is closely associated with intestinal barrier function and the GM,²⁶ which prompted us to investigate the effects of PRP on these parameters. H&E staining revealed an intact colonic tissue structure with neatly arranged villi in the control group. In contrast, the model group exhibited significant inflammatory cell infiltration and disrupted mucosal architecture. Compared to the control group, the PRP intervention group presented lower inflammatory infiltration, which approached that of the control group but was not significantly different from that of the DCF

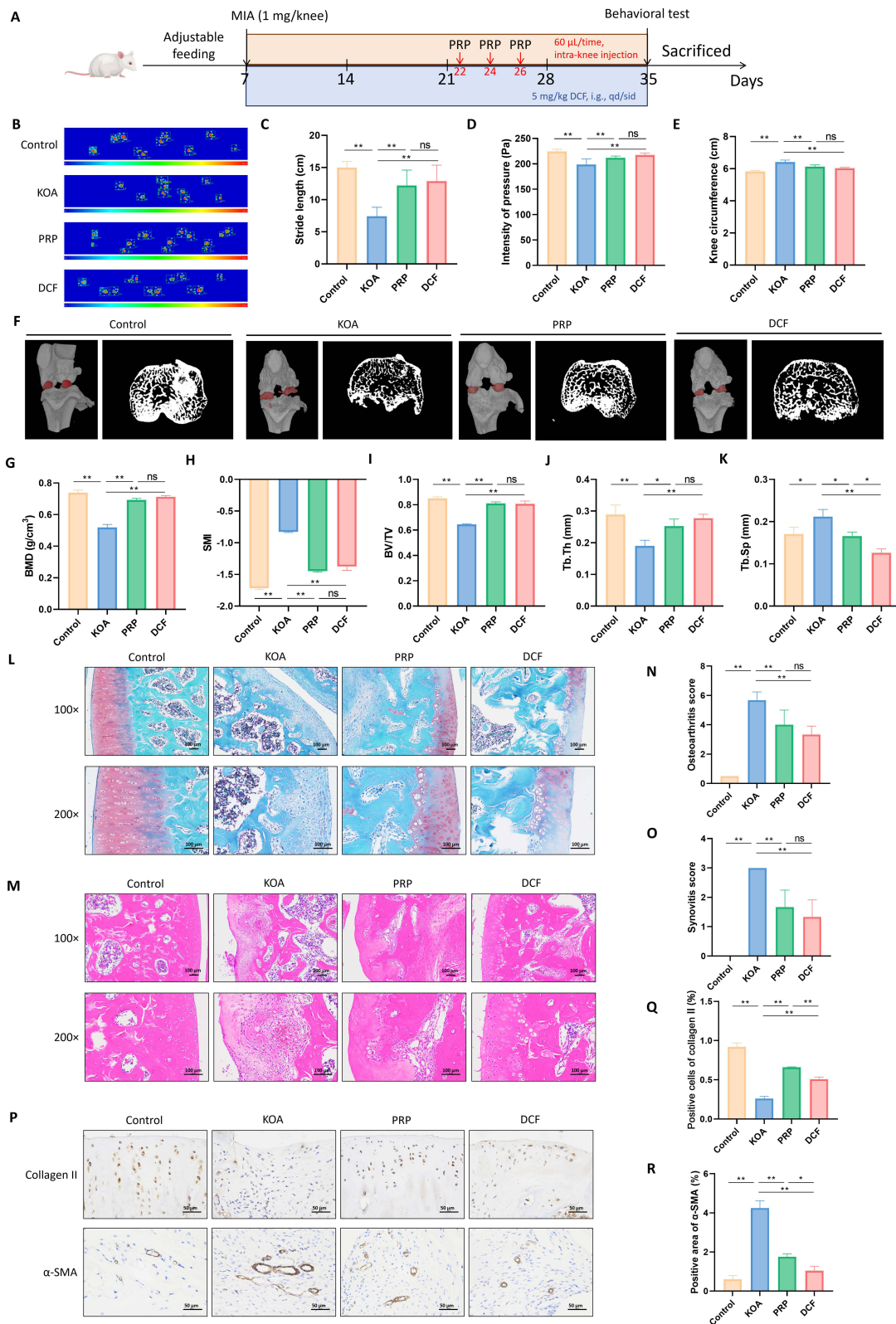


Figure 1 Protective effects of PRP on KOA rats. (A) The flowchart illustrates the establishment of the model; (B) Schematic diagram of gait patterns and footprints; (C) Stride length; (D) Stride pressure; (E) Knee joint circumference; (F) Results of Micro-CT imaging; (G) BMD; (H) SMI; (I) BV/TV; (J) Tb.Th; (K) Tb.Sp; (L) Safranin O-Fast Green staining; (M) H&E staining; (N) Osteoarthritis score; (O) Synovitis Score; (P) IHC detection; (Q and R) Statistical analysis of IHC data. *P < 0.05 and **P < 0.01. **Abbreviations:** ns, not significant.

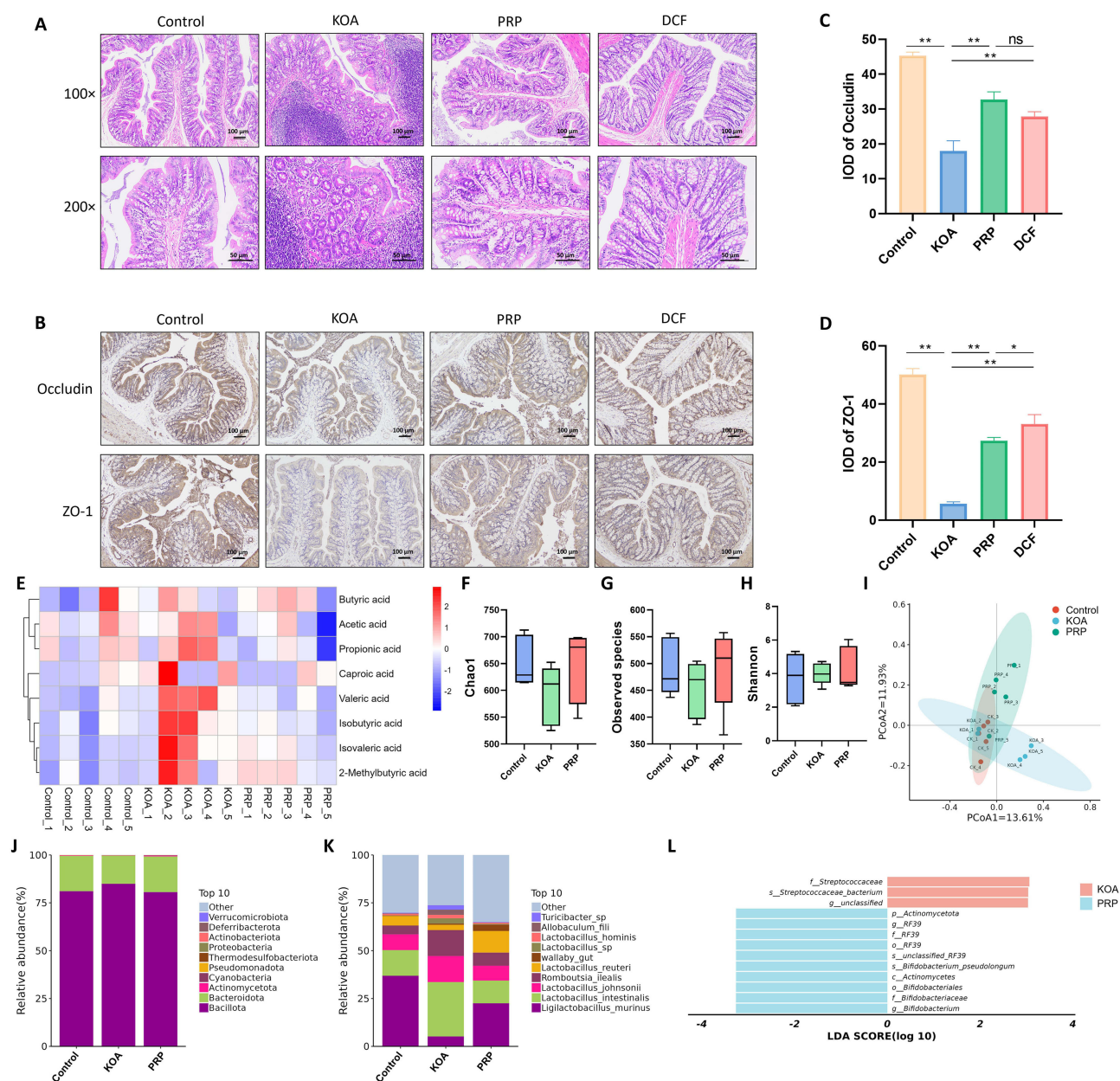


Figure 2 Regulatory effects of PRP on the intestinal barrier and GM in KOA rats. (A) H&E staining of intestinal tissues; (B) Detection of intestinal tissues via immunohistochemical analysis; (C–D) Statistical charts of IHC data; (E) Heatmap of the content of short-chain fatty acids across groups; (F) Chao1 index; (G) Observed species count; (H) Shannon index analysis; (I) Beta diversity analysis; (J) Phylum-level differential changes in fecal samples across groups; (K) Species-level differential changes in fecal samples across groups; (L) LEfSe analysis bar chart of fecal samples. * $P < 0.05$ and ** $P < 0.01$.

Abbreviation: ns, not significant.

group (Figure 2A). Moreover, immunohistochemical analysis of the intestinal barrier function markers Occludin and ZO-1 revealed that their expression was significantly lower in the KOA group, indicating that the integrity of the intestinal barrier was impaired. Following PRP intervention, the expression of Occludin and ZO-1 was restored, which indicated that the intestinal barrier was repaired (Figure 2B–D).

Targeted metabolomics analysis of fecal SCFAs revealed that the levels of butyric acid, acetic acid, and propionic acid decreased in the KOA model group, whereas PRP intervention increased the concentrations of these metabolites (Figure 2E). Analysis of the GM in each group via 16S rRNA gene sequencing revealed that, compared to the control group, the KOA group presented a lower Chao1 index and observed species count, indicating that KOA modeling reduced GM richness. Following PRP intervention, both the Chao1 index and the observed species count increased,

which indicated that microbial richness was restored (Figure 2F–H). Beta diversity analysis revealed that the intergroup distance between the control group and the PRP group was shorter than that between the control group and the KOA group, indicating greater similarity in species composition between the control and PRP groups (Figure 2I). Moreover, community composition analysis revealed that *Ligilactobacillus murinus* was the most abundant bacterium in the GM. Its abundance significantly decreased after KOA modeling, while PRP intervention restored its proportion in the GM (Figure 2J and L). These results indicated that PRP repaired the damaged intestinal barrier function of KOA rats, regulated the richness and composition of the intestinal flora, restored the proportion of key bacterial species, thereby exerting a regulatory effect on KOA rats.

Impact of GM on the Protective Effects of PRP in KOA Rats

The experimental procedure is shown in Figure 3A. Gait analysis revealed that, compared to the pGF group, the pGF-KOA group presented significantly shorter stride length and lower mean pressure. PRP treatment significantly increased both stride length and mean pressure in pGF-KOA rats (Figure 3B–D). Knee joint circumference measurements revealed a significant increase in the model group compared to the germ-free control group, indicating model-associated swelling. PRP intervention reduced the circumference, suggesting that inflammation was alleviated (Figure 3E).

Micro-CT analysis of rat knee joints revealed that, compared to the control group, the KOA model group presented sparse and fractured trabecular bone in the subchondral region, with significantly decreased BMD, BV/TV, and Tb.Th and significantly increased SMI and Tb.Sp. In contrast, the PRP intervention mitigated structural damage, reversed the bone tissue loss observed in the model group, and did not significantly differ from that in the positive control group (Figure 3F–K). Concurrently, histopathological examination of joint tissues via Safranin O-Fast Green staining indicated that, relative to the control group, the model group displayed superficial cartilage fibrillation and loss of proteoglycans, whereas the PRP group presented intensified cartilage matrix staining and significant tissue repair (Figure 3L). H&E staining revealed an intact and well-defined cartilage layer structure in the control group, whereas the model group exhibited disordered cell arrangement and decreased matrix staining. PRP intervention restored the cartilage architecture (Figure 3M). Inflammatory scoring via pathological examination revealed that osteoarthritis and synovitis were significantly elevated in the model group. PRP treatment substantially decreased inflammation levels (Figure 3N and O). The results of IHC analysis revealed significantly lower collagen II levels and greater α -SMA levels in the model group than in the control group. PRP intervention upregulated the expression of collagen II and downregulated the expression of α -SMA (Figure 3P–R). We also compared the therapeutic effects of PRP on KOA rats and pGF-KOA rats. We found that after the intestinal flora was removed, the therapeutic effect of PRP on KOA decreased (Figure 4). These results indicated that PRP alleviated the symptoms of pGF-KOA in rats. However, its efficacy decreased after the intestinal flora was removed, suggesting that the intestinal flora significantly affected the treatment of KOA with PRP.

Effect of PRP on the GM of pGF-KOA Rats

We further analyzed the GM across groups by conducting 16S rRNA gene sequencing. Alpha diversity analysis revealed that, compared to the control group, the KOA group showed a decrease in both the observed species count and the Shannon index. KOA modeling decreased GM richness. After PRP intervention, both the Chao1 index and Shannon index increased, indicating restored microbial richness (Figure 5A–C). Beta diversity analysis revealed a greater intergroup distance between the pGF group and the pGF-PRP group than between the pGF group and the pGF-KOA group, indicating enriched species composition in the pGF-PRP group (Figure 5D). *Ligilactobacillus murinus* was the most abundant species in the GM and was significantly reduced after KOA modeling. PRP intervention restored its proportion in the GM (Figure 5E–G). These results indicated that PRP restored the richness and proportion of key bacterial species in the intestinal flora of pGF-KOA rats.

Fecal Microbiota Derived from PRP Intervention Improves the Condition of KOA Rats

To elucidate the protective role of the GM in PRP-mediated improvement in the progression of KOA, we conducted FMT experiments. As shown in Figure 6A, no significant gait improvement was observed in the KOA-FMT group compared to the gait in the KOA group (Figure 6B). In contrast, rats in the PRP-FMT group and DCF-FMT group exhibited significantly

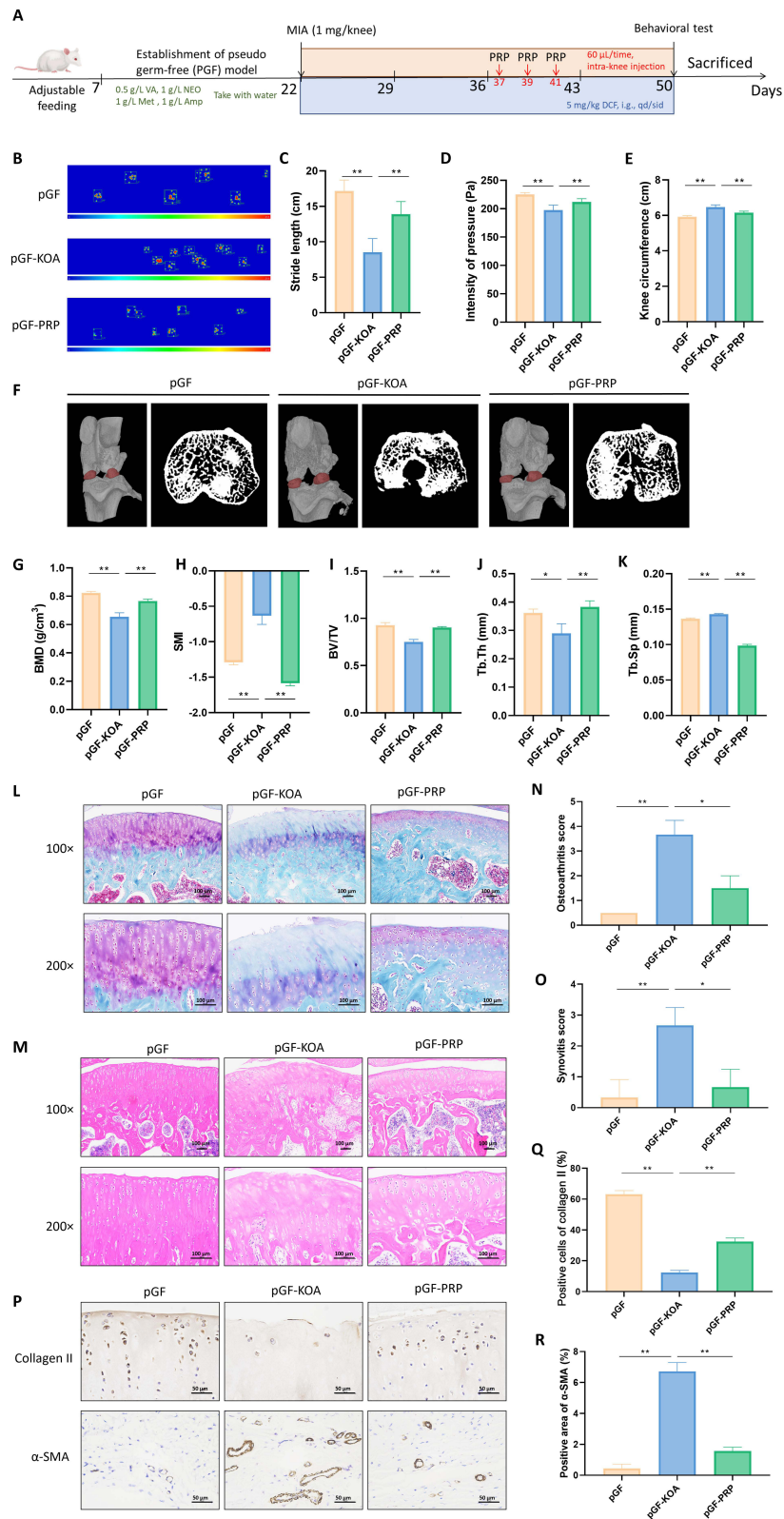


Figure 3 Effect of GM on the protective role of PRP in KOA rats. **(A)** The flowchart illustrates the establishment of the model. **(B)** Gait analysis of each group. **(C)** Stride length. **(D)** Mean paw pressure. **(E)** Knee joint circumference. **(F)** Results of Micro-CT imaging. **(G)** Femoral bone mineral density. **(H)** Structure model index. **(I)** Bone volume fraction. **(J)** Trabecular thickness. **(K)** Trabecular separation. **(L)** Safranin O-fast green staining. **(M)** H&E staining; **(N)** Osteoarthritis score; **(O)** Synovitis score; **(P)** Immunohistochemical detection of the expression of collagen II and α -SMA; **(Q)** and **(R)** Statistical graphs of IHC data. * $P < 0.05$ and ** $P < 0.01$.

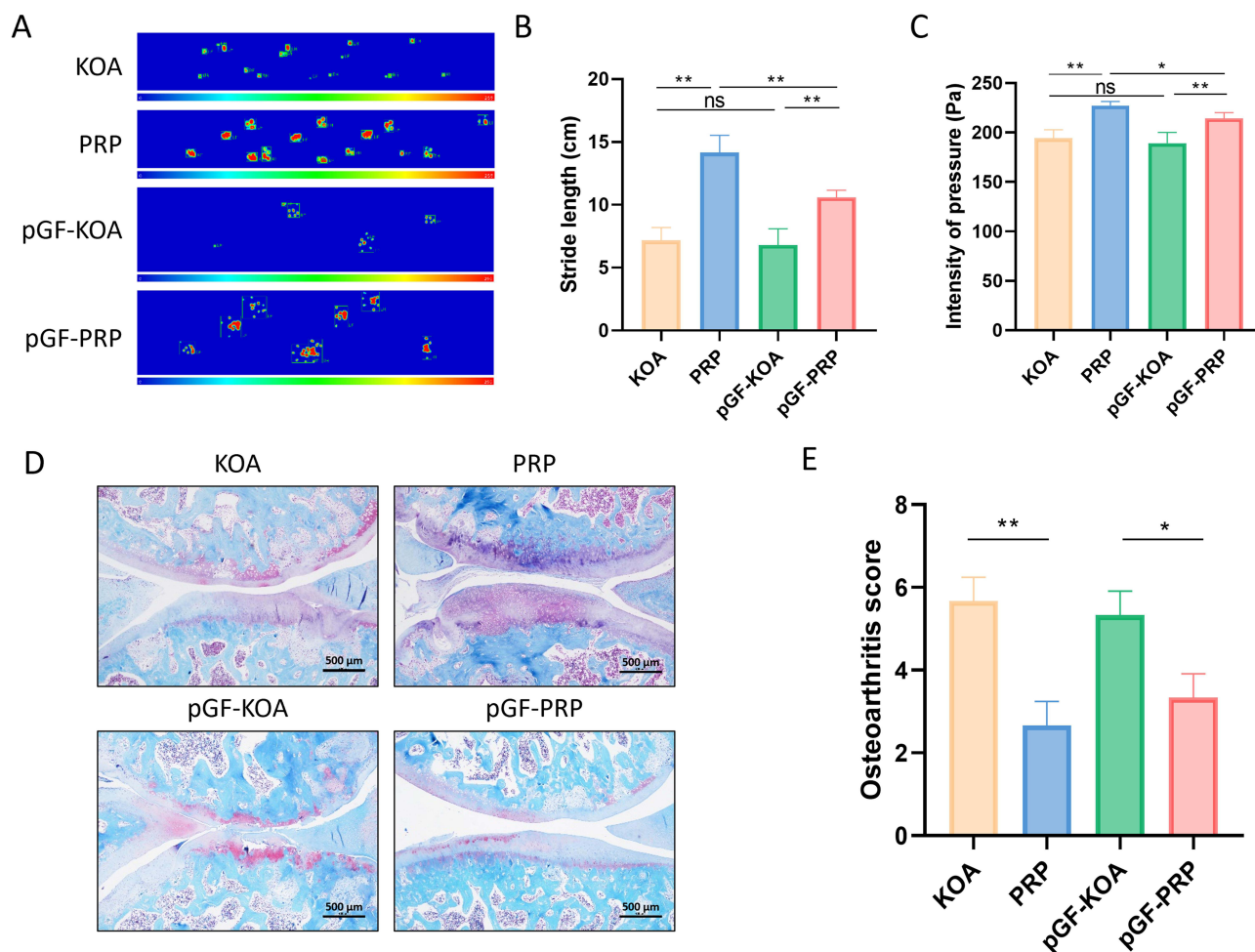


Figure 4 Comparison of the therapeutic effects of PRP in KOA rats and pGF-KOA rats. (A) Gait analysis of each group; (B) Stride length; (C) Mean paw pressure; (D) Safranin O-fast green staining; (E) Osteoarthritis score; * $P < 0.05$ and ** $P < 0.01$.

Abbreviation: ns, not significant.

restored gait, manifested as increased stride length (Figure 6C) and stride pressure values (Figure 6D). Moreover, compared to those in the KOA group, the joints of the rats in the PRP-FMT group and the DCF-FMT group were significantly less swollen (Figure 6E). Further pathological examination of joint tissues revealed through Safranin O-Fast Green staining that the PRP-FMT group and the DCF-FMT group showed marked improvements in superficial cartilage fibrillation and loss of proteoglycans (Figure 6F); additionally, the OARSI scores were reduced (Figure 6G). H&E staining revealed that the PRP-FMT and DCF-FMT groups presented significantly improved disordered chondrocyte populations and cartilage layer structures (Figure 6H), along with considerably lower synovitis scores (Figure 6I). Additionally, the results of the IHC analysis revealed that, compared to those in the control group, the protein expression levels of collagen II and α -SMA in rat cartilage were significantly lower in the KOA group, whereas GM transplantation following PRP intervention significantly increased the protein expression levels of collagen II and α -SMA in recipient rat cartilage (Figures 6J–L). These findings indicated that the GM modulated by PRP intervention exerted a strong therapeutic effect on the progression of KOA. The above results revealed that the intestinal flora after PRP intervention significantly improved gait in KOA rats, reduced joint swelling, repaired cartilage damage, inhibited inflammatory responses, and had a strong therapeutic effect on the progression of KOA.

The Fecal Microbiota Derived from PRP Intervention Improves the GM of KOA Rats

Orthogonal partial least squares-discriminant analysis (OPLS-DA) was performed on the microbiota of the intestinal transplant. The results of the experiments revealed significant differences in the GM, while good reproducibility was

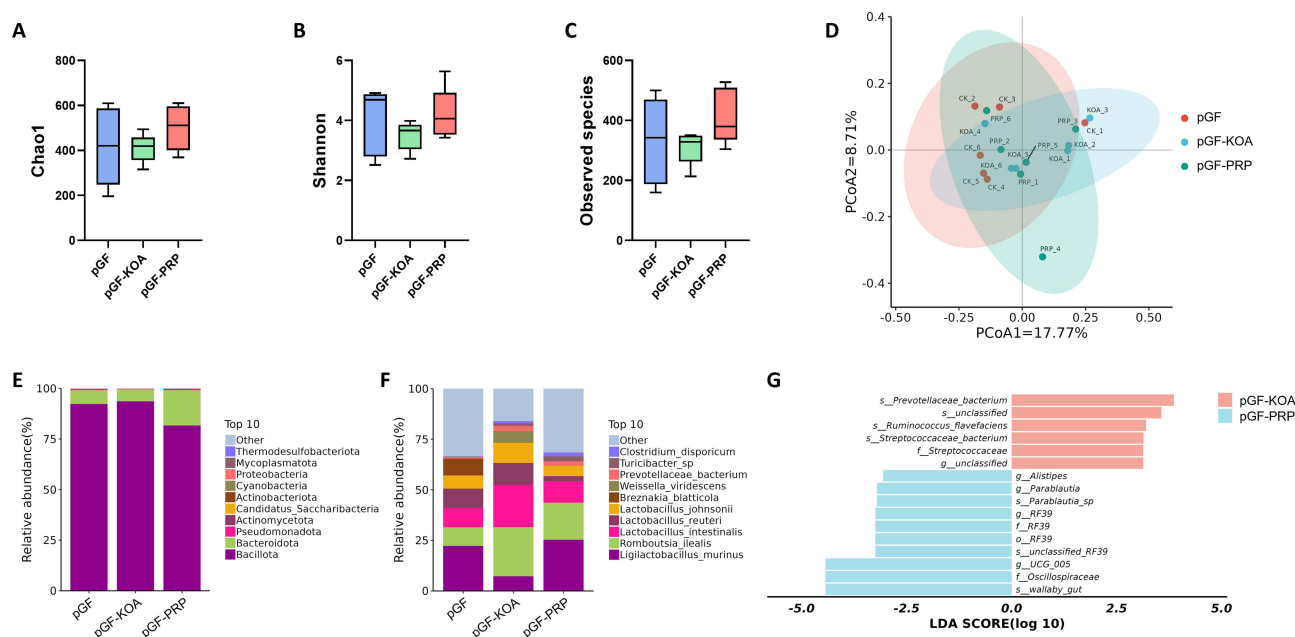


Figure 5 Effect of PRP on the GM of pGF-KOA rats. **(A)** Chao1 index of fecal samples in each group; **(B)** Observed species count; **(C)** Shannon index analysis; **(D)** Beta diversity analysis; **(E)** Phylum-level differential changes in fecal samples across groups; **(F)** Species-level differential changes in fecal samples across groups; **(G)** Bar plot of the LefSe analysis of fecal samples.

observed within each group. After FMT occurred in the model group, the proportions of *Lactobacillus intestinalis*, *Lactobacillus johnsonii*, *Blautia* sp., and *Clostridium disporicum* increased significantly. In contrast, after FMT occurred in the PRP group, the proportions of *Romboutsia ilealis* and *Ruminiclostridium cellulolyticum* increased considerably (Figure 7). These results indicated that the intestinal microbiota derived from PRP treatment restored the richness and proportion of key bacterial species in the intestinal microbiota of KOA rats.

Discussion

We systematically evaluated the therapeutic efficacy of PRP for KOA and its underlying mechanisms. The results demonstrated that intra-articular PRP significantly alleviated MIA-induced KOA progression in rats, as evidenced by improved gait and reduced joint swelling, attenuated subchondral bone loss, and repaired cartilage damage with decreased inflammation scores. These findings corroborate previous studies highlighting PRP's local anti-inflammatory and regenerative potential in OA models.²⁷ Notably, our study further revealed that PRP's therapeutic effects involve systemic modulation of the gut-joint axis.

Platelet-rich plasma (PRP) not only facilitates local tissue repair but also indirectly modulates the progression of KOA by regulating the composition and function of the GM. This systemic role represents a novel extension of its mechanism of action. The microbiota and host immune cells can mutually regulate each other directly or indirectly through the production and release of chemical molecules and signaling factors such as TGF- β .²⁸ During the progression of liver cancer, a higher abundance of bacterial genera such as *Barnesiella* and a lower abundance of beneficial bacteria such as Ruminococcaceae were observed in the GM; concurrently, the plasma levels of endothelin (ET) and VEGF increased.²⁹ Consistent with our findings, KOA rats presented impaired intestinal barrier function and reduced microbial diversity, with significantly decreased α -diversity and β -diversity indices; treatment with PRP reversed this trend. Differential microbiota analysis and LefSe results revealed two key bacterial species regulated by PRP: *Lactobacillus reuteri* (La_re) and *L. murinus* (Li_mu), both of which were found to perform probiotic functions in multiple disease models.^{30–32} Members of the genus *Lactobacillus* can produce SCFAs, and certain SCFAs can inhibit inflammatory cell death in chondrocytes. These bacteria also play a key role in the conversion of primary bile acids to secondary bile acids, potentially further participating in anti-inflammatory modulation. Moreover, the abundance of *L. murinus*, a potential

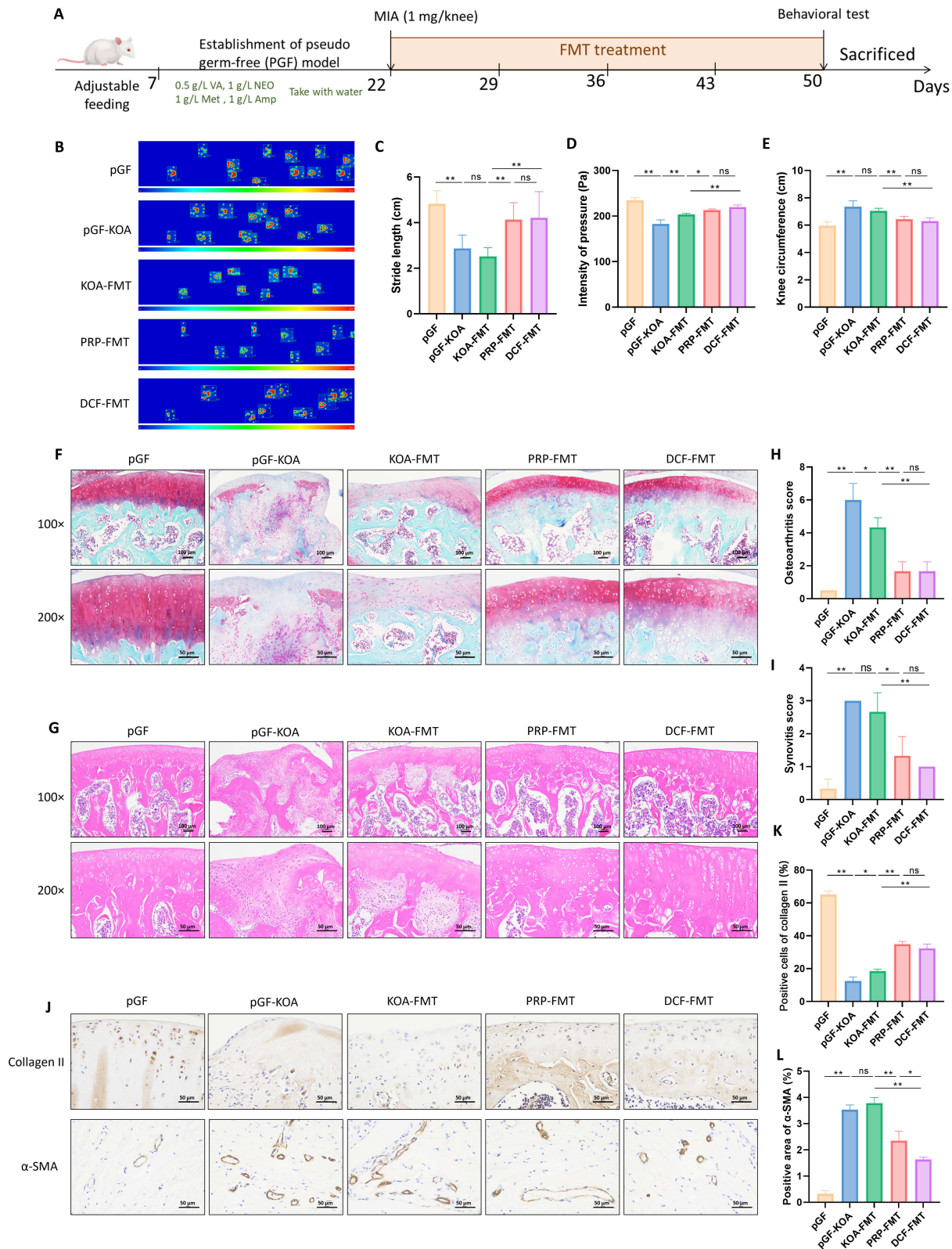


Figure 6 Fecal microbiota derived from PRP intervention improved KOA in rats. **(A)** The flowchart illustrates the establishment of the model; **(B)** Schematic diagram of gait patterns and footprints; **(C)** Stride length; **(D)** Stride pressure; **(E)** Knee joint circumference; **(F)** Safranin O-fast green staining; **(G)** OARSI score; **(H)** H&E staining; **(I)** Synovitis score; **(J)** IHC detection; **(K)** and **(L)** Statistical charts of IHC analysis data. * $P < 0.05$ and ** $P < 0.01$. **Abbreviation:** ns, not significant.

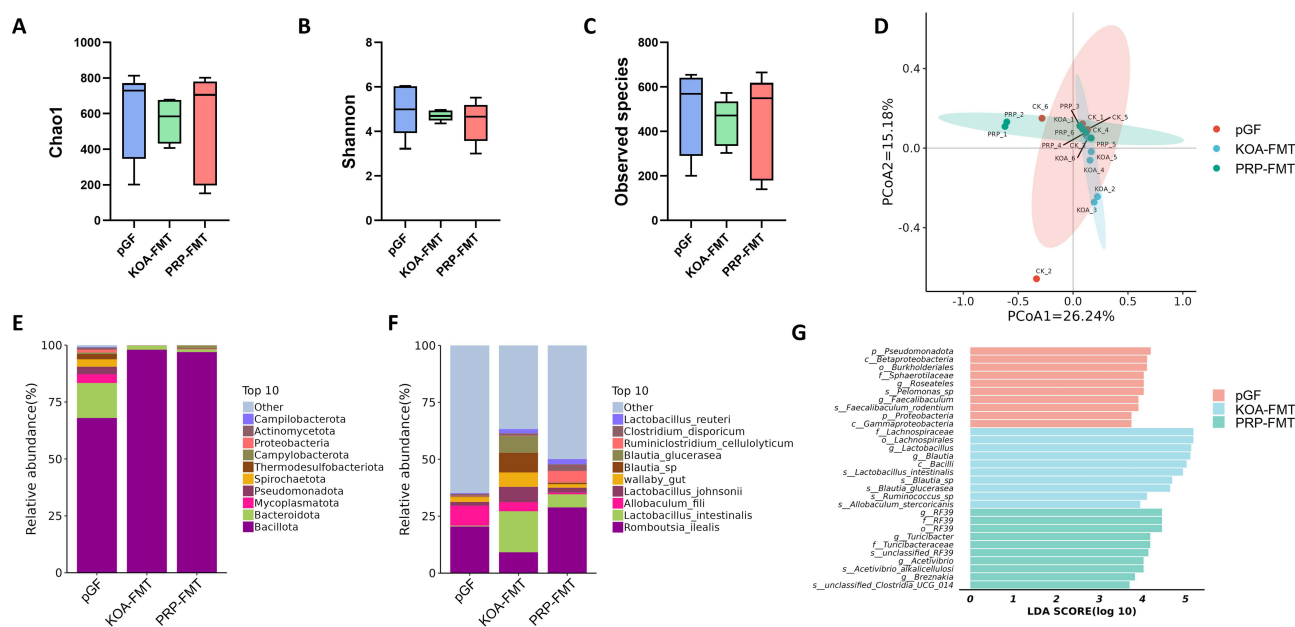


Figure 7 Fecal microbiota derived from PRP intervention improved the GM of KOA rats. (A) Chao1 index of fecal samples across groups; (B) Observed species count; (C) Shannon index analysis; (D) Beta diversity analysis; (E) Phylum-level differential changes in fecal samples across groups; (F) Species-level differential changes in fecal samples across groups; (G) Histogram of the LEfSe analysis for fecal samples.

probiotic, is closely correlated with the health of the intestine, and *L. murinus* extensively participates in host metabolic and immunomodulation processes.³² In LPS-induced inflammation models, the abundance of *Li_mu* consistently decreases,³³ suggesting that it may play an important role in suppressing inflammatory responses. Therefore, PRP may indirectly influence the progression of KOA by regulating the composition and function of the GM. This aligns with the growing concept of a “gut-joint axis” and provides mechanistic support for it, while also distinguishing our work from studies focusing solely on local joint effects.

Beyond the immunomodulatory effects mediated by metabolites such as SCFAs, emerging evidence suggests a more direct physical connection between the gut and joint pathology: the potential translocation of microbes or their components. This concept is strongly supported by studies on the gut-disc axis in intervertebral disc degeneration (IDD). For instance, Liu et al³⁴ demonstrated that patients with IDD exhibit a distinct gut microbiota dysbiosis characterized by an increased abundance of pro-inflammatory phyla such as *Proteobacteria* and *Fusobacteria* alongside altered fecal metabolites like lipids and lipid-like molecules, and proposed that this dysbiosis could compromise the gut epithelial barrier, facilitating the translocation of bacteria or their pro-inflammatory byproducts into the systemic circulation and ultimately reaching the avascular intervertebral disc, thereby contributing to degeneration. This gut-disc axis provides a compelling parallel to the gut-joint axis in KOA. It is plausible that in KOA, a similar mechanism is at play: PRP therapy, by restoring gut eubiosis (eg., increasing *Lactobacillus* abundance as observed in our study), may reinforce intestinal barrier integrity. This reinforcement could, in turn, limit the translocation of pathogens or endotoxins (like LPS) from the gut lumen into the synovial joint, thereby reducing local inflammatory cascades and cartilage degradation. This hypothesized mechanism adds another layer to our understanding of how PRP exerts its systemic therapeutic effects. Notably, PRP showed comparable efficacy to the positive control drug DCF across behavioral, imaging, and histopathological assessments, yet with the potential advantage of also restoring systemic gut homeostasis, a dimension not addressed by conventional NSAID therapy.

Known as the “invisible organ”, the GM plays key roles in immunomodulation. It interacts with inflammatory processes through multiple mechanisms, including the production of probiotic SCFAs^{35,36} and the maintenance of the integrity of the intestinal barrier to prevent pathogen translocation.³⁷ In obese-induced KOA rat models, high levels of LPS, an inflammatory marker, are significantly correlated with altered GM structure and the progression of KOA.³⁸ Moreover, gut dysbiosis is a potential biomarker for multiple inflammatory diseases.^{39–41} Although studies have

suggested an association between GM and KOA, most findings remain confined to correlational analyses, lacking causal evidence. This study provided experimental evidence supporting a causal role of the GM in the development of KOA and the therapeutic action of PRP. The protective effect of PRP on KOA was attenuated after the depletion of the GM, indicating that the GM is involved in the therapeutic mechanism of PRP. Further FMT experiments provided direct evidence that the GM regulates the progression of KOA.

Although this study provided strong evidence that PRP ameliorates the progression of KOA through GM modulation, it had several limitations. First, the PRP preparation used in this study was a freeze-thaw-activated supernatant (releasate), not a standardized platelet concentrate. Key parameters, such as precise platelet and growth factor concentrations, were not characterized, which may affect reproducibility and direct clinical translation. Second, although we identified *L. murinus* as a potentially key bacterial species, monobacterial transplantation experiments were not conducted to validate its function. Finally, we focused primarily on the regulatory effects of PRP on the GM without comprehensively investigating the specific molecular mechanisms through which microbial changes influence KOA. Fourth, the translational relevance of our findings may be constrained by the experimental model. The MIA-induced KOA model represents an acute inflammatory phenotype, which may not fully recapitulate the chronic, low-grade inflammation characteristic of human OA. Additionally, while we propose microbial translocation as a potential mechanism, direct evidence of bacterial components in the synovial joint was not obtained in this study and warrants future investigation. Finally, the use of broad-spectrum antibiotics to create the pGF model, while necessary for depleting the GM, may have off-target effects on host physiology that could independently influence joint pathology. Although our FMT experiments support a specific role for GM, the potential contribution of such antibiotic-induced confounders cannot be entirely ruled out. Future studies should elucidate these mechanisms and employ more chronic OA models to more comprehensively understand the therapeutic effects of PRP on the treatment of KOA.

Conclusions

Platelet-rich plasma (PRP) significantly alleviated MIA-induced progression of KOA in rats by modulating the composition of the GM, enhancing intestinal barrier function, and enriching beneficial microorganisms such as *L. murinus*. Additionally, pGF models and FMT experiments confirmed the key role of the GM in mediating the therapeutic effects of PRP. These findings not only provide novel mechanistic insights into the therapeutic effects of PRP on KOA but also suggest that interventions targeting the GM may represent a new strategy for treating KOA. Future studies should focus on elucidating the interactions between PRP and specific GM and their metabolites, along with their potential in clinical applications.

Data Sharing Statement

The 16S sequencing data and related datasets supporting this study have been deposited in the Science Data Bank (ScienceDB) repository. They can be accessed via the following DOIs:

- (1) Short-Chain Fatty Acids (SCFAs): <https://doi.org/10.57760/sciencedb.28415>
- (2) Microbial *L. murinus* in fecal samples before and after treatment—pseudo-germ-free rat: <https://doi.org/10.57760/sciencedb.28411>
- (3) Microbial in fecal samples before and after PRP intervention—pseudo-germ-free rat: <https://doi.org/10.57760/sciencedb.28405>
- (4) Microbial in fecal samples before and after PRP intervention—common rat: <https://doi.org/10.57760/sciencedb.28403>

Other data are available from the corresponding author upon reasonable request.

Ethics Approval and Consent to Participate

This study was approved by the Animal Ethics Committee of The Second Affiliated Hospital of Harbin Medical University (Ethics Approval Number: SYDW2024-059).

Consent for Publication

All authors agree to the publication of the article.

Author Contributions

All authors made a significant contribution to the work reported, whether that is in the conception, study design, execution, acquisition of data, analysis and interpretation, or in all these areas; took part in drafting, revising or critically reviewing the article; gave final approval of the version to be published; have agreed on the journal to which the article has been submitted; and agree to be accountable for all aspects of the work.

Funding

This work was financially supported by Heilongjiang Province Postdoctoral Research Start-up Fund (No. 21042220098).

Disclosure

The authors report no conflicts of interest in this work.

References

- Hunter DJ, Bierma-Zeinstra S. Osteoarthritis. *Lancet*. 2019;393(10182):1745–1759. doi:10.1016/S0140-6736(19)30417-9
- Zhu S, Qu W, He C. Evaluation and management of knee osteoarthritis. *J Evid Based Med*. 2024;17(3):675–687. doi:10.1111/jebm.12627
- Wongrakpanich S, Wongrakpanich A, Melhado K, et al. A comprehensive review of non-steroidal anti-inflammatory drug use in the elderly. *Aging Dis*. 2018;9(1):143–150. doi:10.14336/AD.2017.0306
- Huizinga JL, Stanley EE, Sullivan JK, et al. Societal cost of opioid use in symptomatic knee osteoarthritis patients in the United States. *Arthritis Care Res*. 2022;74(8):1349–1358. doi:10.1002/acr.24581
- Pereira TV, Jüni P, Saadat P, et al. Viscosupplementation for knee osteoarthritis: systematic review and meta-analysis. *BMJ*. 2022;378:e069722. doi:10.1136/bmj-2022-069722
- Simental-Mendía M, Ortega-Mata D, Acosta-Olivo CA. Platelet-rich plasma for knee osteoarthritis: what does the evidence say? *Drugs Aging*. 2023;40(7):585–603. doi:10.1007/s40266-023-01040-6
- Belk JW, Kraeutler MJ, Houck DA, et al. Platelet-rich plasma versus hyaluronic acid for knee osteoarthritis: a systematic review and meta-analysis of randomized controlled trials. *Am J Sports Med*. 2021;49(1):249–260. doi:10.1177/0363546520909397
- Mishra A, Tummala P, King A, et al. Buffered platelet-rich plasma enhances mesenchymal stem cell proliferation and chondrogenic differentiation. *Tissue Eng Part C Methods*. 2009;15(3):431–435. doi:10.1089/ten.tec.2008.0534
- Araya N, Miyatake K, Tsuji K, et al. Intra-articular injection of pure platelet-rich plasma is the most effective treatment for joint pain by modulating synovial inflammation and calcitonin gene-related peptide expression in a rat arthritis model. *Am J Sports Med*. 2020;48(8):2004–2012. doi:10.1177/0363546520924011
- Wu Q, Yao X, Shan N, et al. Platelet-rich plasma ameliorates cartilage degradation in rat models of osteoarthritis via the OPG/RANKL/RANK system. *Folia Histochem Cytobiol*. 2024;62(3):154–164. doi:10.5603/fhc.100179
- Yan X, Ye Y, Wang L, et al. Platelet-rich plasma alleviates neuropathic pain in osteoarthritis by downregulating microglial activation. *BMC Musculoskelet Disord*. 2024;25(1):331. doi:10.1186/s12891-024-07437-7
- Ticinesi A, Siniscalchi C, Meschi T, et al. Gut microbiome and bone health: update on mechanisms, clinical correlations, and possible treatment strategies. *Osteoporos Int*. 2025;36(2):167–191. doi:10.1007/s00198-024-07320-0
- Guan Z, Jin X, Guan Z, et al. The gut microbiota metabolite capsiate regulate SLC2A1 expression by targeting HIF-1 α to inhibit knee osteoarthritis-induced ferroptosis. *Aging Cell*. 2023;22(6):e13807. doi:10.1111/acer.13807
- Martel J, Chang S-H, Ko Y-F, et al. Gut barrier disruption and chronic disease. *Trends Endocrinol Metab*. 2022;33(4):247–265. doi:10.1016/j.tem.2022.01.002
- Feng Y, Song Y, Zhou J, et al. Recent progress of Lycium barbarum polysaccharides on intestinal microbiota, microbial metabolites and health: a review. *Crit Rev Food Sci Nutr*. 2024;64(10):2917–2940. doi:10.1080/10408398.2022.2128037
- Huang Z, Chen J, Li B, et al. Faecal microbiota transplantation from metabolically compromised human donors accelerates osteoarthritis in mice. *Ann Rheum Dis*. 2020;79(5):646–656. doi:10.1136/annrheumdis-2019-216471
- O-Sullivan I, Natarajan Anbazhagan A, Singh G, et al. Lactobacillus acidophilus mitigates osteoarthritis-associated pain, cartilage disintegration and gut microbiota dysbiosis in an experimental murine OA model. *Biomedicines*. 2022;10(6).
- Longo UG, Lalli A, Bandini B, et al. Role of the gut microbiota in osteoarthritis, rheumatoid arthritis, and spondylarthritis: an update on the gut-joint axis. *Int J Mol Sci*. 2024;25(6):3242. doi:10.3390/ijms25063242
- Kilkenny C, Browne WJ, Cuthill IC, et al. Improving bioscience research reporting: the ARRIVE guidelines for reporting animal research. *PLoS Biol*. 2010;8(6):e1000412. doi:10.1371/journal.pbio.1000412
- Arai T, Suzuki-Narita M, Takeuchi J, et al. Analgesic effects and arthritic changes following intra-articular injection of diclofenac ethalhyaluronate in a rat knee osteoarthritis model. *BMC Musculoskelet Disord*. 2022;23(1):960. doi:10.1186/s12891-022-05937-y
- Zheng YZ, Chen Q-R, Yang H-M, et al. Modulation of gut microbiota by crude mulberry polysaccharide attenuates knee osteoarthritis progression in rats. *Int J Biol Macromol*. 2024;262(Pt 2):129936. doi:10.1016/j.ijbiomac.2024.129936
- Knudsen JK, Michaelsen TY, Bundgaard-Nielsen C, et al. Faecal microbiota transplantation from patients with depression or healthy individuals into rats modulates mood-related behaviour. *Sci Rep*. 2021;11(1):21869. doi:10.1038/s41598-021-01248-9

23. Pritzker KP, Gay S, Jimenez SA, et al. Osteoarthritis cartilage histopathology: grading and staging. *Osteoarthritis Cartilage*. 2006;14(1):13–29. doi:10.1016/j.joca.2005.07.014
24. Krenn V, Morawietz L, Burmester G-R, et al. Synovitis score: discrimination between chronic low-grade and high-grade synovitis. *Histopathology*. 2006;49(4):358–364. doi:10.1111/j.1365-2559.2006.02508.x
25. Ma Y, Ma L, Guo Q, et al. Expression of bone morphogenetic protein-2 and its receptors in epithelial ovarian cancer and their influence on the prognosis of ovarian cancer patients. *J Exp Clin Cancer Res*. 2010;29(1):85. doi:10.1186/1756-9966-29-85
26. Sun C, Zhou X, Guo T, et al. The immune role of the intestinal microbiome in knee osteoarthritis: a review of the possible mechanisms and therapies. *Front Immunol*. 2023;14:1168818. doi:10.3389/fimmu.2023.1168818
27. Osterman C, McCarthy MBR, Cote MP, et al. Platelet-rich plasma increases anti-inflammatory markers in a human coculture model for osteoarthritis. *Am J Sports Med*. 2015;43(6):1474–1484. doi:10.1177/0363546515570463
28. Bauché D, Marie JC. Transforming growth factor β : a master regulator of the gut microbiota and immune cell interactions. *Clin Transl Immunol*. 2017;6(4):e136. doi:10.1038/cti.2017.9
29. Jiang N, Song X, Peng Y-M, et al. Association of disease condition with changes in intestinal flora, and plasma endotoxin and vascular endothelial growth factor levels in patients with liver cancer. *Eur Rev Med Pharmacol Sci*. 2020;24(7):3605–3613. doi:10.26355/eurrev_202004_20822
30. Zhang S, Luo C, Li K, et al. Baicalin alleviates intestinal inflammation and microbial disturbances by regulating Th17/Treg balance and enhancing Lactobacillus colonization in piglets. *J Anim Sci Biotechnol*. 2024;15(1):172. doi:10.1186/s40104-024-01126-0
31. Ma Y, Zhong Y, Tang W, et al. Lactobacillus reuteri ZJ617 attenuates metabolic syndrome via microbiota-derived spermidine. *Nat Commun*. 2025;16(1):877. doi:10.1038/s41467-025-56105-4
32. Chuandong Z, Hu J, Li J, et al. Distribution and roles of Ligilactobacillus murinus in hosts. *Microbiol Res*. 2024;282:127648. doi:10.1016/j.micres.2024.127648
33. Chang W, Guo J, Yang Y, et al. Semen Trigonellae alleviates LPS-induced depressive behavior via enhancing the abundance of Ligilactobacillus spp. *Food Sci Nutr*. 2024;12(11):9414–9427. doi:10.1002/fsn3.4475
34. Liu J, Li T, Jiang T. Characterizing gut microbiota and fecal metabolites in intervertebral disc degeneration: insights into the gut-disc axis. *J Appl Microbiol*. 2025;136(11). doi:10.1093/jambio/ixaf279
35. Mann ER, Lam YK, Uhlig HH. Short-chain fatty acids: linking diet, the microbiome and immunity. *Nat Rev Immunol*. 2024;24(8):577–595. doi:10.1038/s41577-024-01014-8
36. Wang J, Zhu N, Su X, et al. Gut-microbiota-derived metabolites maintain gut and systemic immune homeostasis. *Cells*. 2023;12(5):793. doi:10.3390/cells12050793
37. Di Vincenzo F, Del Gaudio A, Petito V, et al. Gut microbiota, intestinal permeability, and systemic inflammation: a narrative review. *Intern Emerg Med*. 2024;19(2):275–293. doi:10.1007/s11739-023-03374-w
38. Collins KH, Paul HA, Reimer RA, et al. Relationship between inflammation, the gut microbiota, and metabolic osteoarthritis development: studies in a rat model. *Osteoarthritis Cartilage*. 2015;23(11):1989–1998. doi:10.1016/j.joca.2015.03.014
39. Guo X, Huang C, Xu J, et al. Gut microbiota is a potential biomarker in inflammatory bowel disease. *Front Nutr*. 2021;8:818902. doi:10.3389/fnut.2021.818902
40. Moreira de Gouveia MI, Bernalier-Donadille A, Jubelin G. Enterobacteriaceae in the human gut. *Dynamics Ecological Roles Health Disease Biol*. 2024;13(3):142.
41. Huang J, Zhou B, Zhu F, et al. Gut microbiome dysbiosis as a potential biomarker for liver metabolic disorders in neonatal hemolytic jaundice. *BMC Pediatr*. 2025;25(1):337. doi:10.1186/s12887-025-05692-8

Drug Design, Development and Therapy

Publish your work in this journal

Drug Design, Development and Therapy is an international, peer-reviewed open-access journal that spans the spectrum of drug design and development through to clinical applications. Clinical outcomes, patient safety, and programs for the development and effective, safe, and sustained use of medicines are a feature of the journal, which has also been accepted for indexing on PubMed Central. The manuscript management system is completely online and includes a very quick and fair peer-review system, which is all easy to use. Visit <http://www.dovepress.com/testimonials.php> to read real quotes from published authors.

Submit your manuscript here: <https://www.dovepress.com/drug-design-development-and-therapy-journal>

Dovepress
Taylor & Francis Group